



Published in final edited form as:

*J Control Release*. 2019 October ; 311-312: 233–244. doi:10.1016/j.jconrel.2019.09.005.

## Spatiotemporal delivery of basic fibroblast growth factor to directly and simultaneously attenuate cardiac fibrosis and promote cardiac tissue vascularization following myocardial infarction

Zhaobo Fan<sup>a</sup>, Zhaobin Xu<sup>a</sup>, Hong Niu<sup>b</sup>, Yang Sui<sup>b</sup>, Haichang Li<sup>c</sup>, Jianjie Ma<sup>c</sup>, Jianjun Guan<sup>a,b,\*</sup>

<sup>a</sup>Department of Materials Science and Engineering, The Ohio State University, Columbus, OH 43210, United States of America

<sup>b</sup>Department of Mechanical Engineering and Materials Science, Washington University in St. Louis, St. Louis, MO 63130, USA

<sup>c</sup>Department of Surgery, The Ohio State University, Columbus, OH 43210, United States of America

### Abstract

Following myocardial infarction (MI), the destruction of vasculature in the infarcted heart muscle and progression of cardiac fibrosis lead to cardiac function deterioration. Vascularization of the damaged tissue and prevention of cardiac fibrosis represent promising strategies to improve cardiac function. Herein we have developed a bFGF release system with suitable release kinetics to simultaneously achieve the two goals. The release system was based on an injectable, thermosensitive, and fast gelation hydrogel and bFGF. The hydrogel had gelation time < 7 s. It can quickly solidify upon injection into tissue so as to increase drug retention in the tissue. Hydrogel complex modulus can be tuned by hydrogel solution concentration. The complex modulus of 176.6 Pa and lower allowed cardiac fibroblast to maintain its phenotype. Bioactive bFGF was able to gradually release from the hydrogel for 4 weeks. The released bFGF promoted cardiac fibroblast survival under ischemic conditions mimicking those of the infarcted hearts. It also attenuated cardiac fibroblasts from differentiating into myofibroblasts in the presence of TGF $\beta$  when tested in 3D collagen model mimicking the scenario when the bFGF release system was injected into hearts. Furthermore, the released bFGF stimulated human umbilical endothelial cells to form endothelial lumen. After 4 weeks of implantation into infarcted hearts, the bFGF release system significantly increased blood vessel density, decreased myofibroblast density and collagen content, augmented cardiac cell survival/proliferation, and reduced macrophage density. In addition, the bFGF release system significantly increased cardiac function. These results demonstrate that delivery of bFGF with appropriate release kinetics alone may represent an efficient approach to control cardiac remodeling after MI.

\*Corresponding author at: Department of Mechanical Engineering and Materials Science, Washington University in St. Louis, Campus Box 1185, One Brookings Drive, St. Louis, MO 63130, United States of America., jguan22@wustl.edu (J. Guan).

## Keywords

Myocardial infarction; Injectable hydrogel; bFGF; Cardiac fibrosis; Tissue vascularization

---

## 1. Introduction

Myocardial infarction (MI) is a major cardiovascular disease that affects millions of people in the western countries. Following MI, the destruction of vasculature in the affected cardiac muscle leads to extensive cell death. The dead tissue then undergoes progressive adverse remodeling. Revascularization to revitalize the dead tissue has been considered as an effective approach to attenuate the adverse remodeling and improve cardiac function [1–5]. Pro-angiogenic therapy is commonly used for revascularization [6–10]. It involves delivery of angiogenic growth factors such as bFGF, VEGF, and PDGF into infarcted area to stimulate angiogenesis. However, systemic delivery has low efficacy due to short half-life of the growth factors [6–10]. Controlled and local delivery of these growth factors using microspheres and hydrogels may improve the efficacy [6–10]. Yet a significant loss of growth factors may occur during the delivery due to low retention of microspheres and hydrogels in the heart tissue. Increase of growth factor retention in the tissue after delivery is expected to improve the efficacy of vascularization. This may be achieved by using fast gelation hydrogels as growth factor carriers. Previous studies have demonstrated that fast gelation hydrogels can be quickly immobilized in tissues after injection so as to improve drug retention [11–13].

Cardiac fibrosis also occurs after MI. It is characterized by excessive deposition of extracellular matrix (ECM) in the infarcted area, causing tissue stiffening and limiting the systolic and diastolic functions of the heart. While the fibrotic tissue formed initially has protective effect to prevent the infarcted heart from rupture, continued cardiac fibrosis leads to a decrease in cardiac function [14–18]. Myofibroblasts, formed primarily through TGF $\beta$  binding to TGF $\beta$  receptors (TGF $\beta$ R) on cardiac fibroblasts (TGF $\beta$  pathway), are responsible for cardiac fibrosis. To prevent cardiac fibrosis from progressing, it is crucial to inhibit TGF $\beta$  pathway-mediated myofibroblast formation. However, this cannot be readily achieved by existing therapies. Current therapies are mostly focused on the systemic delivery of TGF $\beta$  inhibitors or anti-TGF $\beta$  antibodies to decrease the amount of active TGF $\beta$  in the heart [19–24]. These drugs do not block TGF $\beta$  from binding to TGF $\beta$ R. Therefore, they cannot fundamentally prevent myofibroblast formation. For this reason, current therapies can only decrease cardiac fibrosis, but cannot essentially prevent cardiac fibrosis. TGF $\beta$ R inhibitors have the potential to block TGF $\beta$  from binding to TGF $\beta$ R on cardiac fibroblasts. While various TGF $\beta$ R inhibitors exist, most are used for cancer therapy [25,26]. One of the potential challenges in using these inhibitors for anti-fibrotic therapy is their relatively high toxicity [25,26]. Employing nontoxic growth factors for anti-fibrotic therapy may address the toxicity issue. Previous studies have shown that bFGF and HGF had anti-fibrotic effect when delivered into infarcted hearts. [27] [28] The anti-fibrotic effect of bFGF has long been attributed to increased angiogenesis in infarcted hearts. Until recently, its direct contribution has been identified, i.e., bFGF is capable of inhibiting TGF $\beta$ -induced cardiac fibroblast differentiation into myofibroblast [29].

The objective of this work was to simultaneously vascularize the infarcted heart tissue and attenuate cardiac fibrosis in order to improve cardiac function. To achieve the goal, the pro-angiogenic and anti-fibrotic growth factor bFGF was delivered into infarcted hearts. While bFGF has pro-angiogenic and anti-fibrotic effects, it is yet to determine how bFGF release profiles can be modulated to simultaneously inhibit myofibroblast formation and promote endothelial cell morphogenesis. We show in this report that the two goals can be achieved by appropriate bFGF release kinetics. To address the low retention associated with growth factor delivery, a fast gelation hydrogel that can solidify within 7 s at 37 °C was used as bFGF carrier. When using a hydrogel as the growth factor carrier for anti-fibrotic therapy, it is essential that the hydrogel itself does not induce myofibroblast formation. This requires that the hydrogel to have appropriate stiffness as matrix stiffness itself can stimulate fibroblasts to differentiate into myofibroblasts. [30,31] In this report, the hydrogel stiffness was modulated to not induce myofibroblast formation.

## 2. Materials and methods

### 2.1. Materials

All materials were purchased from Sigma-Aldrich unless otherwise stated. N-isopropylacrylamide (NIPAAm, TCI) was recrystallized before use. 2-hydroxyethyl methacrylate (HEMA, TCI) was passed through an inhibitor remover (Sigma Aldrich) to remove the inhibitors. Heparin sulfate (Alfa Aesar), recombinant human bFGF (peprotech), bFGF Elisa Kit (peprotech), collagen I solution (Fisher Scientific), Dulbecco's Modified Eagle Medium (DMEM) powder (Fisher Scientific), 3,6-dimethyl-1,4-dioxane-2,5-dione, sodium methoxide, and triethylamine (Fisher-Scientific) were used as received.

### 2.2. Synthesis of hydrogel polymer

The hydrogel polymer was based on NIPAAm, HEMA, and a macromer acrylate-oligolactide (AOLA). AOLA was synthesized through ring-opening polymerization of 3,6-dimethyl-1,4-dioxane-2,5-dione followed by esterification with acryloyl chloride using our established approach [11]. Structure of the macromer was confirmed by <sup>1</sup>H NMR, and the number of lactide units per macromer was 2.57. The hydrogel polymer was polymerized by free radical polymerization. In brief, under the protection of nitrogen, NIPAAm (7.44 g, 65.8 mmol), HEMA (0.996 g, 7.7 mmol), and AOLA (0.816 g, 3.1 mmol) were dissolved in 1,4-dioxane. Benzoyl peroxide (37.3 mg, 0.154 mmol) was then added into the solution. The polymerization was conducted at 70 °C for 24 h. The polymer solution was precipitated in hexane, and further purified by THF/diethyl ether. The synthesized polymer had a NIPAAm/HEMA/AOLA ratio of 86.0/10.4/3.6 as determined by <sup>1</sup>H NMR spectrum.

### 2.3. Characterization of hydrogel complex modulus

Hydrogel solutions with concentrations of 2, 4, 7 and 10 wt% were prepared by dissolving the hydrogel polymer in Dubecco's modified phosphate-buffered saline (DPBS). The rheological test was conducted in an AR-G2 rheometer equipped with a Peltier plate (TA Instruments). The radius of smooth geometry was 8 mm, and the gap height was 1 mm. The testing was performed in a temperature range of 11 °C to 37 °C with a rate of 2 °C/min. The

strain and oscillatory frequency were 2% and 1 Hz, respectively. TA Rheology Advantage TM software was utilized for data acquisition and analysis.

#### 2.4. Cardiac fibroblast phenotype on hydrogel surface

The hydrogel solutions with concentrations of 2, 4, 7, and 10 wt% were sterilized under UV light for 30 min. Each solution was then added into 24-well plates (300  $\mu$ L/well). After 10 min of incubation at 37  $^{\circ}$ C, the supernatant was removed, and the rat cardiac fibroblasts were seeded on the hydrogel surface. The seeding density was  $1 \times 10^6$  cells/mL. The cells were cultured at 37  $^{\circ}$ C with 5% CO<sub>2</sub> and 21% O<sub>2</sub>. DMEM supplemented with 10% fetal bovine serum (FBS) and 1% penicillin-streptomycin was used as culture medium. The samples were collected after 1 and 7 days of incubation.

The phenotype of cardiac fibroblasts on the hydrogel surface was characterized at the protein level by immunohistochemistry. To perform immunohistological staining, the samples were fixed by 4% formaldehyde solution followed by permeabilization with 0.1% Triton X-100 and blocking with 10% goat serum. The samples were stained with primary antibody  $\alpha$ SMA overnight, and secondary antibody Alexa Fluor 546 goat-anti-rat IgG for 1 h. Hoechst 33328 was used to stain cell nuclei. Fluorescent images were taken with a confocal microscope (Olympus FV1000).

#### 2.5. Release of bFGF from the hydrogel

Hydrogel solution with concentration of 4 wt% was used to fabricate bFGF release system. bFGF stock solution was added to reach the final concentration of 10 and 50  $\mu$ g/mL, respectively. To preserve the bioactivity of the encapsulated bFGF, heparin sulfate (1 wt%) was also added into the solutions [32]. 200  $\mu$ L of bFGF-loaded hydrogel solution was then incubated in a 37  $^{\circ}$ C water bath for gelation. After 30 min, supernatant was collected and replaced by 200  $\mu$ L DPBS. bFGF release was conducted in a 37  $^{\circ}$ C water bath for 4 weeks. At each pre-determined time point, the release medium was collected and replaced with equal volume of fresh DPBS. The content of released bFGF was measured using a bFGF ELISA kit [33].

#### 2.6. Bioactivity of released bFGF

Bioactivity of the released bFGF was evaluated by proliferation assay of rat cardiac fibroblasts. The cell suspension was seeded in a 96-well plate at a density of  $2 \times 10^5$  cells/mL. After 24 h, the culture medium was replaced with the collected release medium supplemented with 0.5% FBS. Following 48 h of culture, cell viability was assessed by MTT assay [34]. 1 ng/mL bFGF solution, and the release medium collected from the hydrogel without bFGF were used as controls. Relative cell viability was quantified by normalizing MTT absorbance of the release medium to that of the 1 ng/mL bFGF.

#### 2.7. Effect of bFGF release on cardiac fibroblast phenotype in the presence of TGF $\beta$

To determine the effect of released bFGF on cardiac fibroblast phenotype, a 3D model of collagen gel seeded with cardiac fibroblasts and injected with hydrogel/bFGF was used. This model mimics the scenario where hydrogel/bFGF is injected into heart [35]. In brief, type I rat tail collagen solution (2.0 mg/mL) was mixed with DMEM, 10% FBS, and 0.1 M NaOH.

Cardiac fibroblast suspension was mixed with the collagen gel solution at a density of  $2 \times 10^6$  cells/mL. The mixture was pipetted into a 48-well plate (600  $\mu$ L/well) and incubated at 37 °C for gelation. After 45 min, 300  $\mu$ L hydrogel/bFGF solution was injected into each collagen gel at 5 points. The culture medium was supplemented with 5 ng/mL of TGF $\beta$ 1. The samples were collected after one day of culture in a hypoxic incubator (1% O<sub>2</sub>, 5% CO<sub>2</sub>, and 37 °C). The phenotype of cardiac fibroblasts was characterized at the mRNA level by real-time RT-PCR, and protein level by immunohistochemistry.

To prepare the samples for real-time RT-PCR, TRIzol™ reagent (ThermoFisher) was utilized to extract RNA. The RNA concentration was determined by Nanodrop (ThermoFisher). One microgram of RNA was utilized for cDNA synthesis by a High Capacity cDNA Reverse Transcription kit (ABI). Primers  $\beta$ -actin (F: ACTCTGTGTGGATTGGT GGC; R: AGCTCAGTAACAGTCCGCCT), alpha smooth muscle actin ( $\alpha$ SMA, F: CATCAGGAACCTCGAGAAGC; R: TCGGATACTTCAGGGTC AGG), Collagen 1A1 (F: TTCACCTACAGCACGCTTGT; R: TTGGGATGG AGGGAGTTTAC), and CTGF (F: ACTGGTATTTGCAACTGCTTTGG; R: GCGACCCACACAAGGGTCT) were used. Real-time RT-PCR was conducted with Maxima SYBR Green/fluorescein master mix on LightCycler® 480 System (Roche). Fold difference was calculated using a standard Ct method. The immunohistochemical staining was performed using the approach described above. The myofibroblast density was calculated as number of  $\alpha$ SMA+ cells per area of each image.

## 2.8. Effect of bFGF release on endothelial lumen formation

To determine the effect of released bFGF on endothelial cell function, tube formation assay was performed. The collagen gel described above was used for the assay. After gelation, human umbilical vein endothelial cells (HUVECs) were seeded on the gel surface at a density of  $6 \times 10^4$  cells/mL. 300  $\mu$ L hydrogel solution or Hydrogel/bFGF solution was then injected into each collagen gel at 5 points. Five collagen gels were used for each group. 5 ng/mL of TGF $\beta$ 1 was added to the culture medium. The samples were incubated in a hypoxia incubator (1% O<sub>2</sub>, 5% CO<sub>2</sub>, and 37 °C) for 24 h. The tube formation was determined by immunohistochemistry. The samples were stained with vWF (rabbit-anti-rat) antibody and Alexa 546 secondary antibody, respectively. Cell nuclei were stained by Hoechst 33328. The vWF positive endothelial lumens were counted from images.

## 2.9. Myocardial infarction and implantation of hydrogel encapsulated with bFGF

All the animal experiments were conducted in line with the National Institutes of Health guide for handling laboratory animals. The animal protocol was approved by the Institutional Animal Care and Use Committee of the Ohio State University. Sprague-Dawley rats aged 10–12 weeks (~ 200 g) were used. MI was induced by ligation of left anterior descending coronary artery based on our previously established method [11,13]. After 30 min, hydrogel solution (Hydrogel group) or bFGF encapsulated hydrogel solution (Hydrogel/bFGF group) was injected into the apical, proximal, lateral, and septal wall regions bordering the infarct, and the center of the infarct with 40  $\mu$ L/injection. The animals without injection was used as control. Each group had at least 6 animals.

## 2.10. Cardiac function analysis by echocardiography

Four weeks following injection, the cardiac function of animals was evaluated by echocardiography. [11,13] Two dimensional and M-mode echocardiographic images were captured and analyzed using Vevo 2100 High-Resolution in vivo imaging system and MS400 transducer (VisualSonics, Toronto, ON, Canada). Images were obtained in a parasternal short and long axis view. In the echocardiographic images, the dimensions of the left ventricle were measured in a short axis view during the diastole and systole. Ejection fraction (EF) and fractional shortening (FS) were quantified.

## 2.11. Histological and immunohistochemical analyses

Rat hearts were harvested 4 weeks after surgery. The tissues were fixed in a freshly prepared 4% paraformaldehyde overnight. The fixed tissues were then embedded in paraffin, and sequentially sectioned at 4  $\mu\text{m}$  thickness. The sections were then stained with hematoxylin and eosin (H&E), and Picrosirius Red (PSR). In H&E images, the thicknesses of infarcted left ventricle and normal left ventricle were measured by Image J [36]. The relative thickness was calculated as the ratio of thickness of infarcted area to that of normal area. Collagen types I and III were identified from PSR staining using polarized light microscopy [37,38]. The percent area of collagen within the remote and MI regions was determined from images ( $n = 5$ ) using threshold image analysis with Image J software [37].

For immunohistochemical staining, the tissue sections were stained with  $\alpha\text{SMA}$ , vWF, Ki67, and F4/80 antibodies, respectively [39]. Myofibroblasts were identified as  $\alpha\text{SMA}^+$  cells that were not co-localized with vWF+ endothelial cells. The  $\alpha\text{SMA}^+$  and spindle-shape cells with stress fiber were myofibroblasts. The matured blood vessels were lumens with  $\alpha\text{SMA}^+$  and vWF+ cells. The Ki67+ cells and F4/80+ cells in the infarcted area were proliferating cells and macrophages, respectively.

## 3. Results

### 3.1. Effect of hydrogel modulus on cardiac fibroblast phenotype

The hydrogel modulus was tailored by hydrogel solution concentration. Four hydrogel solutions with concentrations of 2%, 4%, 7%, and 10% were used. The 4  $^{\circ}\text{C}$  solutions can be readily injected through a 26G needle, and can solidify within 7 s at 37  $^{\circ}\text{C}$ . Rheological tests demonstrate that the increase of solution concentration from 2% to 4% to 7% increased complex modulus from 78.3 Pa to 156.5 Pa to 176.6 Pa at 37  $^{\circ}\text{C}$  (Fig. 1). Further increase of concentration to 10% remarkably increased the complex modulus to 756.1 Pa (Fig. 1).

To determine the effect of hydrogel modulus on cardiac fibroblast differentiation into myofibroblast, the cells were seeded on the hydrogel surface. After 1 day of culture, the cells were stained for  $\alpha\text{SMA}$ , a marker for myofibroblast (Fig. 2). All of the cells on the hydrogels with complex moduli of 78.3 Pa – 176.6 Pa did not express  $\alpha\text{SMA}$ , demonstrating that these moduli maintained cardiac fibroblast phenotype. The increase of complex modulus to 756.1 Pa led to myofibroblast formation as all of the cells were  $\alpha\text{SMA}^+$ .

### 3.2. Release kinetics of bFGF and bioactivity of the released bFGF

The hydrogel with complex modulus of 156.5 Pa (concentration 4%) was further used to encapsulate bFGF for controlled release of bFGF. This hydrogel can be better handled during encapsulation and cell culture than the hydrogel with complex modulus of 78.3 Pa. bFGF was able to continuously release from the hydrogel for 4 weeks (Fig. 3A). The release exhibited a tri-phasic pattern, i.e., a burst release during the first day, a sustained release from days 1 to 7, and a nearly linear yet slow release after day 7. The release kinetics was dependent on the amount of bFGF loaded into the hydrogel. At each time point, the concentration of released bFGF was greater in the group with 50  $\mu\text{g/mL}$  of bFGF than that with 10  $\mu\text{g/mL}$  of bFGF.

The bioactivity of released bFGF was assessed through its stimulatory effect on the survival of cardiac fibroblast under the low oxygen condition mimicking that of the infarcted heart. 1 ng/mL bFGF was used as a positive control. Fig. 3B shows that this concentration significantly increased cell viability compared to the release medium collected from the group without bFGF (Control group). The cardiac fibroblasts cultured in the medium with released bFGF had significantly greater viability than those cultured in 1 ng/mL bFGF, demonstrating that the bFGF released from the hydrogel loaded with 10  $\mu\text{g/mL}$  and 50  $\mu\text{g/mL}$  bFGF remained bioactive.

### 3.3. Effect of bFGF release on cardiac fibroblast phenotype

To determine the effect of bFGF release on cardiac fibroblast phenotype, a 3D collagen model seeded with cardiac fibroblasts, injected with Hydrogel/bFGF, and cultured in the presence of TGF $\beta$  was used (Fig. 4A). This model mimics the scenario when the Hydrogel/bFGF is injected into an infarcted heart where the upregulated TGF $\beta$  is mainly responsible for myofibroblast formation. Following 1 day of culture, the Collagen/Hydrogel group had greater expressions of  $\alpha\text{SMA}$ , CTGF, and collagen 1A1 at the mRNA level than the Collagen group (Fig. 4B). After injection of Hydrogel/bFGF into collagen (Collagen/Hydrogel/bFGF group), these expressions were remarkably decreased ( $p < .01$  for all 3 genes, Collagen vs. Collagen/Hydrogel/bFGF, Collagen/Hydrogel vs. Collagen/Hydrogel/bFGF, Fig. 4B).

Further characterization of cardiac fibroblast phenotype was conducted at the protein level utilizing immunohistochemistry (Fig. 4C). In the Collagen group, most of the cells were  $\alpha\text{SMA}^+$ . Injection of hydrogel into the collagen did not change cell phenotype as 97% of the cells remained  $\alpha\text{SMA}^+$ . Interestingly, in the group injected with hydrogel/bFGF, the percentage of  $\alpha\text{SMA}^+$  cells was significantly decreased to 26% ( $p < .01$ , Collagen vs. Collagen/Hydrogel/bFGF, Collagen/Hydrogel vs. Collagen/Hydrogel/bFGF). The above results demonstrate that the released bFGF was capable of inhibiting TGF $\beta$ -induced cardiac myofibroblast formation.

### 3.4. Efficacy of bFGF delivery system in inducing endothelial cell tube formation

bFGF has proangiogenic effect. To determine whether the released bFGF can also effectively stimulate endothelial cell lumen formation, the above collagen model with HUVEC seeded

on the surface, and injected with Hydrogel/bFGF was used (Fig. 5A). After 2 days of culture, only few HUVECs migrated.

and sprouted to form lumens in the Collagen and Collagen/Hydrogel groups (Fig. 5B). The injection of Hydrogel/bFGF greatly induced the lumen formation where the lumen density was significantly higher than the Collagen and Collagen/Hydrogel/bFGF groups ( $p < .0001$ , Fig. 5C). These results suggest that the released bFGF was able to efficiently promote angiogenesis.

### 3.5. Effect of bFGF release on left ventricle remodeling

To examine the effect of bFGF release on the left ventricle remodeling, the infarcted hearts were injected with hydrogel loaded with bFGF (Hydrogel/bFGF) 30 min following MI. The infarcted hearts injected with hydrogel (Hydrogel), or without treatment (MI) were used as controls. Four weeks after MI, apparent wall thinning was found for the MI group (Fig. 6). The walls of the Hydrogel and Hydrogel/bFGF groups appear to be thicker (Fig. 6). Relative wall thickness was quantified as the ratio of the wall thickness at infarcted zone to that of the healthy left ventricles. The thickness of the MI group was decreased to ~30% after 4 weeks (Fig. 7). The injection of Gel group significantly increased wall thickness ( $p < .05$ , Fig. 7). It was further increased after injection of Hydrogel/bFGF group ( $p < .05$ , Hydrogel vs. Hydrogel/bFGF, Fig. 7). These results demonstrate that injection of Hydrogel and Hydrogel/bFGF attenuated left ventricle remodeling.

### 3.6. Effect of bFGF release on angiogenesis and cardiac fibrosis in infarcted tissue

bFGF promotes tissue angiogenesis. To determine whether bFGF released from the hydrogel was sufficient to stimulate vessel formation in the infarcted area, the density of vWF+ vessels was quantified. The MI and Hydrogel groups exhibited similar vessel density ( $p > .05$ , Fig. 8), indicating that the hydrogel alone did not induce vessel formation. In contrast, the injection of Hydrogel/bFGF remarkably increased the vessel density ( $p < .001$  for MI vs. Hydrogel/bFGF, and Hydrogel vs. Hydrogel/bFGF). These results demonstrate that the hydrogel released adequate bFGF to promote angiogenesis.

In the infarcted hearts, myofibroblasts are responsible for cardiac fibrosis that is featured by increased collagen deposition. To evaluate the effect of bFGF release on cardiac fibrosis, myofibroblast density and total collagen content in the infarcted area were quantified (Figs. 8 & 9). Myofibroblasts are identified as those  $\alpha$ SMA+ cells that are not colocalized with vWF+ endothelial cells [11,13]. The injection of hydrogel did not significantly induce myofibroblast formation as the Hydrogel group had similar myofibroblast density as the MI group ( $p > .05$ ). The myofibroblast density was significantly decreased in the Hydrogel/bFGF group compared to the Hydrogel and MI groups ( $p < .001$  for MI vs. Hydrogel/bFGF, and Hydrogel vs. Hydrogel/bFGF). Picrosirius Red staining was used to identify two major collagens (I and III) in the infarcted tissue (Fig. 9). The Hydrogel/bFGF group exhibited significantly lower total collagen content than the Hydrogel and MI groups ( $p < .05$  for MI vs. Hydrogel/bFGF, and Hydrogel vs. Hydrogel/bFGF). The above results show that the released bFGF effectively attenuated cardiac fibrosis by inhibiting cardiac fibroblast formation and decreasing collagen deposition.



### 3.7. Effect of bFGF release on host cell proliferation

bFGF is capable of promoting cell survival and proliferation under ischemic conditions [34]. To determine whether the cells in the infarcted area were able to proliferate in response to the released bFGF, ki67 staining was performed (Fig. 10). The MI group had ki67+ cell density of 201.6 #/mm<sup>2</sup>. The injection of hydrogel did not significantly increase the density ( $p > .1$ ). In contrast, the density was significantly augmented after the injection of Hydrogel/bFGF group ( $p < .05$  for hydrogel/bFGF vs. MI, and  $p < .05$  for Hydrogel/bFGF vs. Hydrogel), indicating that the released bFGF promoted host cell proliferation.

### 3.8. Efficacy of bFGF release in reducing tissue inflammation

F4/80 staining was utilized to evaluate the effect of bFGF release on tissue inflammation. The MI group exhibited the greatest inflammation as demonstrated by the highest F4/80+ cell density (Fig. 11). The injection of hydrogel did not significantly increase F4/80+ cell density ( $p > .1$  Hydrogel vs. MI). The lowest inflammation was found for the Hydrogel/bFGF group where the F4/80+ cell density was significantly lower than that in the Hydrogel and MI groups ( $p < .05$  for Hydrogel/bFGF vs. Hydrogel, and  $p < .01$  for Hydrogel/bFGF vs. MI).

### 3.9. Efficacy of bFGF release in improving cardiac function

Cardiac function (EF and FS) was evaluated by echocardiography after 4 weeks of implantation (Fig. 12). The EF and FS were remarkably decreased for the MI group compared to the Sham group ( $p < .01$ ). Injection of hydrogel only (Hydrogel group) into the infarcted area significantly increased EF and FS ( $p < .05$ , Hydrogel vs. MI). The EF and FS were further significantly increased after injection of the Hydrogel/bFGF group ( $p < .05$ , Hydrogel/bFGF vs. Hydrogel). These results demonstrate that the released bFGF increased cardiac function and attenuated cardiac remodeling.

## 4. Discussion

In this work, a bFGF release system was developed to directly and simultaneously promote angiogenesis and attenuate cardiac fibrosis following MI. *Re*-establishment of destructed vasculature and attenuation of cardiac fibrosis represent effective strategies to increase cardiac function. bFGF is known to stimulate angiogenesis by promoting endothelial cell morphogenesis. bFGF also has direct effect on tissue fibrosis by inhibiting TGF $\beta$ -induced fibroblast differentiation into myofibroblast [29]. Yet our knowledge is still lacking on how the bFGF release can be modulated to concurrently promote endothelial cell morphogenesis, and inhibit cardiac fibroblast differentiation into myofibroblast. In this report, we have shown that bFGF release system with appropriate release kinetics can achieve the goals.

To develop bFGF release system, a NIPAAm-based injectable and thermal sensitive hydrogel with fast gelation rate was used as carrier. PNIPAAm solution exhibits temperature-dependent hydrophilicity and hydrophobicity that change abruptly when the temperature is increased to the thermal transition temperature. At this temperature, the polymer chains undergo a coil-to-globule transition. Therefore, PNIPAAm is precipitated out from the solution to form a solid gel [40,41]. At 37 °C, the hydrogel solution can solidify

within 7s. The advantage of quick gelation is that the hydrogel as well as the encapsulated drug can be readily immobilized in the tissue without substantial leaking. Slow gelation rate hydrogels have the disadvantage of leaking out during tissue injection [12]. Besides serving as a drug carrier, the injected hydrogel can also provide mechanical and structural support to the infarcted tissue.

One of the considerations when selecting drug carrier is that the carrier itself has suitable stiffness that does not induce cardiac fibroblast differentiation into myofibroblast. Matrix stiffness has been shown to regulate fibroblast phenotype [30,31]. High stiffness matrix promotes myofibroblast activation through PI3K/AKT signaling pathway while soft matrix maintains the quiescent phenotype of fibroblast [42]. To determine suitable stiffness for the current hydrogel that can keep the fibroblast phenotype, hydrogels with 4 different complex moduli were fabricated by using solutions with different concentrations. The complex modulus was ranged from 78.3 to 756.1 Pa (Fig. 1). The cells on the hydrogel with 756.1 Pa complex modulus turned cardiac fibroblasts into  $\alpha$ SMA+ myofibroblasts (Fig. 2), but not on the hydrogels with complex modulus of 78.3–176.6 Pa. These results demonstrate that hydrogel with complex modulus of 176.6 Pa or lower is suitable for bFGF delivery.

The bFGF release system was able to gradually release bioactive bFGF for 28 days (Fig. 3). The release exhibited a tri-phasic pattern: a burst release in day 1, a sustained release from day 1 to day 7, and an approximately linear but slow release from day 7 to day 28. This release profile is consistent with previous work using a PNIPAAm-based hydrogel as delivery vehicle [34]. The burst release is possibly due to the diffusion of bFGF from surface layer of the hydrogel. The slower and sustained release is likely attributed to the interactions among heparin, bFGF, and hydrogel. Heparin contains negative charges including carboxylic and sulfate groups, which may interact with amine and amide groups in bFGF, and hydroxyl and amide groups from the hydrogel by electrostatic interaction and hydrogen bonding. In addition, the amine, amide and hydroxyl groups in the bFGF and hydrogel can form hydrogen bonding. These different interactions among heparin, bFGF and hydrogel allowed bFGF to gradually release out from the hydrogel instead of burst release. Similar approach has been used to achieve sustained release of proteins even small molecules from gelatin hydrogel. The enhanced interactions of gelatin and proteins or small molecules by host-guest complexation and hydrogen bonding enabled them to release for > 2 weeks [43,44]. The bFGF release kinetics was dose-dependent. The hydrogel loaded with 50  $\mu$ g/mL bFGF released greater amount of bFGF at each time point than that loaded with 10  $\mu$ g/mL bFGF (Fig. 3).

Following MI, the harsh low nutrient and oxygen conditions lead to cell death. To investigate how released bFGF affects cardiac fibroblast survival under the low nutrient and oxygen conditions mimicking that of the infarcted heart, the cells were cultured at 1% oxygen and 1% FBS conditions, and treated with the released bFGF. At each time point the released bFGF significantly improved cardiac fibroblast survival (Fig. 3B). Consistent with in vitro results, the in vivo implantation of the bFGF release system into infarcted hearts promoted cell proliferation as the ki67+ cell density was significantly greater in the Hydrogel/bFGF group than that in the Hydrogel and MI groups (Fig. 10). While cardiac fibroblasts may not be the only cells that were ki67+, these cells represent one of the major cell types in the

infarcted area. The *in vitro* and *in vivo* studies demonstrate that the released bFGF was sufficient for promoting cardiac fibroblast survival under ischemic conditions. The enhanced cell proliferation *in vivo* may also be the result of enhanced vascularization in the infarcted area as the Hydrogel/bFGF group had significantly higher density of vessels than the MI and Hydrogel groups (Fig. 8). In addition, the released bFGF may augment cardiac cell survival before vascularization is established.

In the infarcted hearts, the upregulated TGF $\beta$  differentiates cardiac fibroblast into myofibroblast leading to cardiac fibrosis. bFGF has been found to decrease tissue fibrosis initiated by TGF $\beta$ . [45–47] This is partially a result of bFGF attenuating cardiac fibroblasts from differentiating into myofibroblasts. [29] To determine whether the released bFGF was sufficient to prevent cardiac fibroblast differentiation, a 3D collagen gel model seeded with cardiac fibroblasts, treated with TGF $\beta$ , and injected with Hydrogel/bFGF was used. 3D collagen model has been utilized to mimic the microenvironment of cardiac ECM to study fibroblast phenotype in previous reports [48,49]. After 1 day of culture, the number of  $\alpha$ SMA+ myofibroblasts was remarkably decreased compared to the Collagen group and collagen injected with hydrogel only group (Collagen/Hydrogel group) (Fig. 4). In addition, the hydrogel injected into the collagen gel did not induce myofibroblast formation as the number of  $\alpha$ SMA+ myofibroblasts was similar in the Collagen group and Collagen/Hydrogel group. This is consistent with Fig. 2 where the hydrogel with the same modulus did not differentiate cardiac fibroblasts into myofibroblasts. After 4 weeks of *in vivo* implantation, the released bFGF significantly decreased the density of myofibroblasts in the infarcted area (Fig. 8). As a result, collagen deposition was reduced (Fig. 9). These results demonstrate that the amount of released bFGF was able to effectively inhibit cardiac fibroblasts to differentiate into myofibroblasts, and attenuate cardiac fibrosis.

Vascularization of infarcted hearts has been considered as an effective approach to improve cardiac function. bFGF is known to stimulate angiogenesis by promoting endothelial cell morphogenesis [50]. To determine whether the released bFGF can induce endothelial cell to form lumen *in vitro*, HUVECs were seeded on the surface of collagen gel injected with Hydrogel/bFGF, and cultured under low oxygen and nutrient conditions mimicking those of the infarcted hearts. The released bFGF remarkably increased HUVEC lumen density compared with the control (Collagen) and hydrogel injection alone (Collagen/Hydrogel, Fig. 5). After 4 weeks of injection of the bFGF release system into infarcted hearts, the released bFGF stimulated blood vessel formation. The vessel density was remarkably greater in the Hydrogel/bFGF group than in the Hydrogel and MI group (Fig. 8). The above results demonstrate that the released bFGF was capable of promoting endothelial cell morphogenesis *in vitro*, and angiogenesis *in vivo*.

MI leads to left ventricular wall thinning [51,52]. Four weeks post-MI, the MI group exhibited a remarkably low wall thickness (Figs. 6 & 7). Injection of hydrogel alone into the infarcted area significantly increased wall thickness (Figs. 6 & 7). It is likely that the soft hydrogel acted as a bulking agent. Similar results were found in previous studies [39,53,54]. The injection of bFGF delivery system further significantly augmented the wall thickness (Figs. 6 & 7). The increased wall thickness (Figs. 6 & 7), improved cell survival/proliferation (Fig. 10), decreased cardiac fibrosis (Figs. 8 & 9), and enhanced tissue

vascularization (Fig. 8) after delivery of bFGF release system in the infarcted hearts led to the increase of cardiac function including EF and FS (Fig. 12). The cardiac function in the Hydrogel/bFGF group was significantly greater than that in the Hydrogel and MI groups (Fig. 12). In addition, the Hydrogel group exhibited higher EF and FS than MI group. This increase may be resulted from structural support of the hydrogel [39,53]. It is also possible that the injected hydrogel effectively decreased the elevated wall stress [55].

bFGF has been delivered into infarcted hearts after MI by using either injectable hydrogels [56–59] or cardiac patches [60,61] as carriers. In these studies, the reduced fibrosis and increased cardiac function were considered as the result of increased vascularization. In this study, we demonstrate that the anti-fibrotic effect of bFGF in infarcted hearts is resulted from bFGF inhibition of cardiac fibroblasts to differentiate into myofibroblasts. This work is advantageous over previous studies in using bFGF carrier that does not induce cardiac fibroblast differentiation into myofibroblast. Prior reports did not consider the effect of carrier mechanical properties on the myofibroblast formation as matrix stiffness itself may stimulate the differentiation of cardiac fibroblast. The results from this work also demonstrate that bFGF release systems capable of releasing sufficient amount of bFGF can simultaneously improve cell survival/proliferation, attenuate cardiac fibrosis, stimulate tissue vascularization, and improve cardiac function.

The developed bFGF release system may be delivered into the infarcted hearts during coronary revascularization after MI [4]. In this work, acute MI model was used. This model has been widely utilized to evaluate therapeutic efficacy of cell, biomaterials and drug therapies [4,5,54,62,63]. Yet the major limitation of acute MI model is its relatively low clinical relevance.

## 5. Conclusions

An injectable, biodegradable, thermosensitive, and quick gelation hydrogel that can preserve cardiac fibroblast phenotype was used to deliver bFGF into infarcted hearts. The developed bFGF delivery system can release bFGF for at least 28 days, and released bFGF remained bioactive. In vitro, the bFGF release system with appropriate release kinetics simultaneously prevented cardiac fibroblasts differentiation into myofibroblasts, stimulated endothelial cell morphogenesis, and promoted cardiac fibroblast survival when tested in the conditions mimicking those of the infarcted hearts. In vivo, the bFGF release system significantly reduced cardiac fibrosis, promoted blood vessel formation, and improved cardiac function.

## Acknowledgments

This work was supported by US National Institutes of Health (R01HL138175, R01HL138353, R01EB022018, R01AG056919, and R21EB021896), and National Science Foundation (1708956). We appreciate the help from Minghuan Fu, Xuanyou Liu, Yunyan Duan and Pei-Hui Lin at Ohio State University.

## References

- [1]. Lindsey ML, Gannon J, Aikawa M, Schoen FJ, Rabkin E, Lopresti-Morrow L, Crawford J, Black S, Libby P, Mitchell PG, Lee RT, Selective matrix metalloproteinase inhibition reduces left

- ventricular remodeling but does not inhibit angiogenesis after myocardial infarction, *Circulation* 105 (6) (2002) 753–758. [PubMed: 11839633]
- [2]. Apple KA, Yarbrough WM, Mukherjee R, Deschamps AM, Escobar PG, Mingoia JT, Sample JA, Hendrick JW, Dowdy KB, McLean JE, Stroud RE, O’Neill TP, Spinale FG, Selective targeting of matrix metalloproteinase inhibition in post-infarction myocardial remodeling, *J. Cardiovasc. Pharmacol* 47 (2) (2006) 228–235. [PubMed: 16495760]
  - [3]. Lindsey ML, MMP induction and inhibition in myocardial infarction, *Heart Fail. Rev* 9 (1) (2004) 7–19. [PubMed: 14739764]
  - [4]. Eckhouse SR, Purcell BP, McGarvey JR, Lobb D, Logdon CB, Doviak H, O’Neill JW, Shuman JA, Novack CP, Zellars KN, Pettaway S, Black RA, Khakoo A, Lee T, Mukherjee R, Gorman JH, Gorman RC, Burdick JA, Spinale FG, Local hydrogel release of recombinant TIMP-3 attenuates adverse left ventricular remodeling after experimental myocardial infarction, *Sci. Transl. Med* 6 (223) (2014) 223ra21.
  - [5]. Purcell BP, Lobb D, Charati MB, Dorsey SM, Wade RJ, Zellars KN, Doviak H, Pettaway S, Logdon CB, Shuman JA, Freels PD, Gorman JH 3rd, Gorman RC, Spinale FG, Burdick JA, Injectable and bioresponsive hydrogels for on-demand matrix metalloproteinase inhibition, *Nat. Mater* 13 (6) (2014) 653–661. [PubMed: 24681647]
  - [6]. Cochain C, Channon KM, Silvestre JS, Angiogenesis in the infarcted myocardium, *Antioxid. Redox Signal* 18 (9) (2013) 1100–1113. [PubMed: 22870932]
  - [7]. Devezza L, Choi J, Yang F, Therapeutic angiogenesis for treating cardiovascular diseases, *Theranostics* 2 (8) (2012) 801–814. [PubMed: 22916079]
  - [8]. Formiga FR, Tamayo E, Simon-Yarza T, Pelacho B, Prosper F, Blanco-Prieto MJ, Angiogenic therapy for cardiac repair based on protein delivery systems, *Heart Fail. Rev* 17 (3) (2012) 449–473. [PubMed: 21979836]
  - [9]. Awada HK, Johnson NR, Wang Y, Sequential delivery of angiogenic growth factors improves revascularization and heart function after myocardial infarction, *J. Control. Release* 207 (2015) 7–17. [PubMed: 25836592]
  - [10]. Segers VF, Lee RT, Protein therapeutics for cardiac regeneration after myocardial infarction, *J. Cardiovasc. Transl. Res* 3 (5) (2010) 469–477. [PubMed: 20607468]
  - [11]. Fan Z, Xu Z, Niu H, Gao N, Guan Y, Li C, Dang Y, Cui X, Liu XL, Duan Y, Li H, Zhou X, Lin PH, Ma J, Guan J, An injectable oxygen release system to augment cell survival and promote cardiac repair following myocardial infarction, *Sci. Rep* 8 (1) (2018) 1371. [PubMed: 29358595]
  - [12]. Niu H, Li X, Li H, Fan Z, Ma J, Guan J, Thermosensitive, fast gelling, photo-luminescent, highly flexible, and degradable hydrogels for stem cell delivery, *Acta Biomater* 83 (2019) 96–108. [PubMed: 30541703]
  - [13]. Fan Z, Fu M, Xu Z, Zhang B, Li Z, Li H, Zhou X, Liu X, Duan Y, Lin PH, Duann P, Xie X, Ma J, Liu Z, Guan J, Sustained release of a peptide-based matrix Metalloproteinase-2 inhibitor to attenuate adverse cardiac Remodeling and improve cardiac function following myocardial infarction, *Biomacromolecules* 18 (9) (2017) 2820–2829. [PubMed: 28731675]
  - [14]. Dobaczewski M, de Haan JJ, Frangogiannis NG, The extracellular matrix modulates fibroblast phenotype and function in the infarcted myocardium, *J. Cardiovasc. Transl. Res* 5 (6) (2012) 837–847. [PubMed: 22956156]
  - [15]. Gonzalez A, Ravassa S, Beaumont J, Lopez B, Diez J, New targets to treat the structural remodeling of the myocardium, *J. Am. Coll. Cardiol* 58 (18) (2011) 1833–1843. [PubMed: 22018293]
  - [16]. van den Borne SW, Diez J, Blankesteyn WM, Verjans J, Hofstra L, Narula J, Myocardial remodeling after infarction: the role of myofibroblasts, *Nat. Rev. Cardiol* 7 (1) (2010) 30–37. [PubMed: 19949426]
  - [17]. Yarbrough WM, Mukherjee R, Stroud RE, Rivers WT, Oelsen JM, Dixon JA, Eckhouse SR, Ikonomidis JS, Zile MR, Spinale FG, Progressive induction of left ventricular pressure overload in a large animal model elicits myocardial remodeling and a unique matrix signature, *J. Thorac. Cardiovasc. Surg* 143 (1) (2012) 215–223. [PubMed: 22056365]
  - [18]. Kong P, Christia P, Frangogiannis NG, The pathogenesis of cardiac fibrosis, *Cell. Mol. Life Sci* 71 (4) (2014) 549–574. [PubMed: 23649149]

- [19]. Bujak M, Frangogiannis NG, The role of TGF-beta signaling in myocardial infarction and cardiac remodeling, *Cardiovasc. Res* 74 (2) (2007) 184–195. [PubMed: 17109837]
- [20]. Cunnington RH, Nazari M, Dixon IM, C-ski, Smurf2, and Arkadia as regulators of TGF-beta signaling: new targets for managing myofibroblast function and cardiac fibrosis, *Can. J. Physiol. Pharmacol* 87 (10) (2009) 764–772. [PubMed: 19898560]
- [21]. Kuwahara F, Kai H, Tokuda K, Kai M, Takeshita A, Egashira K, Imaizumi T, Transforming growth factor-beta function blocking prevents myocardial fibrosis and diastolic dysfunction in pressure-overloaded rats, *Circulation* 106 (1) (2002) 130–135. [PubMed: 12093782]
- [22]. Lei B, Hitomi H, Mori T, Nagai Y, Deguchi K, Mori H, Masaki T, Nakano D, Kobori H, Kitaura Y, Nishiyama A, Effect of efonidipine on TGF-beta1-induced cardiac fibrosis through Smad2-dependent pathway in rat cardiac fibroblasts, *J. Pharmacol. Sci* 117 (2) (2011) 98–105. [PubMed: 21897055]
- [23]. Takai S, Jin D, Sakaguchi M, Katayama S, Muramatsu M, Sakaguchi M, Matsumura E, Kim S, Miyazaki M, A novel chymase inhibitor, 4-[1-[[bis-(4-methyl-phenyl)methyl]-carbonyl]-3-(2-ethoxy-benzyl)-4-oxo-azetidine-2-yl]-benzoic acid (BCEAB), suppressed cardiac fibrosis in cardiomyopathic hamsters, *J. Pharmacol. Exp. Ther* 305 (1) (2003) 17–23. [PubMed: 12649348]
- [24]. Zhou DX, Li ZH, Zhang LW, Zhan CY, Inhibitory effect of tanshinone II a on TGF II-beta 1-induced cardiac fibrosis, *J Huazhong U Sci-Med* 32 (6) (2012) 829–833.
- [25]. Akhurst RJ, Hata A, Targeting the TGFbeta signalling pathway in disease, *Nat. Rev. Drug Discov* 11 (10) (2012) 790–811. [PubMed: 23000686]
- [26]. Nagaraj NS, Datta PK, Targeting the transforming growth factor-beta signaling pathway in human cancer, *Expert Opin. Investig. Drugs* 19 (1) (2010) 77–91.
- [27]. Salimath AS, Phelps EA, Boopathy AV, Che PL, Brown M, Garcia AJ, Davis ME, Dual delivery of hepatocyte and vascular endothelial growth factors via a protease-degradable hydrogel improves cardiac function in rats, *PLoS One* 7 (11) (2012) e50980.
- [28]. Banquet S, Gomez E, Nicol L, Edwards-Levy F, Henry JP, Cao R, Schapman D, Dautreux B, Lallemand F, Bauer F, Cao Y, Thuillez C, Mulder P, Richard V, Brakenhielm E, Arteriogenic therapy by intramyocardial sustained delivery of a novel growth factor combination prevents chronic heart failure, *Circulation* 124 (9) (2011) 1059–1069. [PubMed: 21824923]
- [29]. Svystonyuk DA, Ngu JM, Mewhort HE, Lipon BD, Teng G, Guzzardi DG, Malik G, Belke DD, Fedak PW, Fibroblast growth factor-2 regulates human cardiac myofibroblast-mediated extracellular matrix remodeling, *J. Transl. Med* 13 (1) (2015) 147. [PubMed: 25948488]
- [30]. Jacot JG, McCulloch AD, Omens JH, Substrate stiffness affects the functional maturation of neonatal rat ventricular myocytes, *Biophys. J* 95 (7) (2008) 3479–3487. [PubMed: 18586852]
- [31]. Forte G, Pagliari S, Ebara M, Uto K, Tam JK, Romanazzo S, Escobedo-Lucea C, Romano E, Di Nardo P, Traversa E, Aoyagi T, Substrate stiffness modulates gene expression and phenotype in neonatal cardiomyocytes in vitro, *Tissue Eng. A* 18 (17–18) (2012) 1837–1848.
- [32]. Faham S, Hileman RE, Fromm JR, Linhardt RJ, Rees DC, Heparin structure and interactions with basic fibroblast growth factor, *Science (New York, N.Y.)* 271 (5252) (1996) 1116–1120.
- [33]. Shi YH, Bingle L, Gong LH, Wang YX, Corke KP, Fang WG, Basic FGF augments hypoxia induced HIF-1-alpha expression and VEGF release in T47D breast cancer cells, *Pathology* 39 (4) (2007) 396–400. [PubMed: 17676480]
- [34]. Li Z, Guo X, Guan J, A thermosensitive hydrogel capable of releasing bFGF for enhanced differentiation of mesenchymal stem cell into cardiomyocyte-like cells under ischemic conditions, *Biomacromolecules* 13 (6) (2012) 1956–1964. [PubMed: 22578081]
- [35]. Gudur M, Rao RR, Hsiao YS, Peterson AW, Deng CX, Stegemann JP, Noninvasive, quantitative, spatiotemporal characterization of mineralization in three-dimensional collagen hydrogels using high-resolution spectral ultrasound imaging, *Tissue Eng Part C Methods* 18 (12) (2012) 935–946. [PubMed: 22624791]
- [36]. Duan AQ, Lock MC, Perumal SR, Darby JR, Soo JY, Selvanayagam JB, Macgowan CK, Seed M, Morrison JL, Feasibility of detecting myocardial infarction in the sheep fetus using late gadolinium enhancement CMR imaging, *J. Cardiovasc. Magn. Reson* 19 (1) (2017) 69. [PubMed: 28903760]

- [37]. Junqueira LC, Bignolas G, Brentani RR, Picosirius staining plus polarization microscopy, a specific method for collagen detection in tissue sections, *Histochem. J* 11 (4) (1979) 447–455. [PubMed: 91593]
- [38]. Namba T, Tsutsui H, Tagawa H, Takahashi M, Saito K, Kozai T, Usui M, Imanaka-Yoshida T Imaizumi, A. Takeshita, Regulation of fibrillar collagen gene expression and protein accumulation in volume-overloaded cardiac hypertrophy, *Circulation* 95 (10) (1997) 2448. [PubMed: 9170409]
- [39]. Dekker S, van Geemen D, van den Bogaerd AJ, Driessen-Mol A, Aikawa E, Smits AIPM, Sheep-Specific Immunohistochemical Panel for the Evaluation of Regenerative and Inflammatory Processes in Tissue-Engineered Heart Valves, *Front. Cardiovasc. Med* 5 (2018) 105. [PubMed: 30159315]
- [40]. Wu C, Wang X, Globule-to-coil transition of a single Homopolymer chain in solution, *Phys. Rev. Lett* 80 (18) (1998) 4092–4094.
- [41]. Okano T, Bae YH, Jacobs H, Kim SW, Thermally on-off switching polymers for drug permeation and release, *J. Control. Release* 11 (1) (1990) 255–265.
- [42]. Wang H, Tibbitt MW, Langer SJ, Leinwand LA, Anseth KS, Hydrogels preserve native phenotypes of valvular fibroblasts through an elasticity-regulated PI3K/AKT pathway, *Proc. Natl. Acad. Sci* 110 (48) (2013) 19336–19341. [PubMed: 24218588]
- [43]. Feng Q, Xu J, Zhang K, Yao H, Zheng N, Zheng L, Wang J, Wei K, Xiao X, Qin L, Bian L, Dynamic and cell-infiltratable hydrogels as injectable carrier of therapeutic cells and drugs for treating challenging bone defects, *ACS Central Sci* 5 (3) (2019) 440–450.
- [44]. Xu J, Feng Q, Lin S, Yuan W, Li R, Li J, Wei K, Chen X, Zhang K, Yang Y, Wu T, Wang B, Zhu M, Guo R, Li G, Bian L, Injectable stem cell-laden supra-molecular hydrogels enhance in situ osteochondral regeneration via the sustained co-delivery of hydrophilic and hydrophobic chondrogenic molecules, *Biomaterials* 210 (2019) 51–61. [PubMed: 31075723]
- [45]. Hata Y, Ishikawa H, Ueki T, Kajii TS, Tamaoki S, Tsuruga E, Sawa Y, Taniguchi K, Quantitative evaluation of myofibroblast apoptosis during wound healing in rat palate after post-operative administration of basic fibroblast growth factor (bFGF), *Acta Odontol. Scand* 71 (6) (2013) 1501–1507. [PubMed: 23445304]
- [46]. Gallego-Muñoz P, Ibares-Frías L, Valsero-Blanco MC, Cantalapiedra-Rodríguez R, Merayo-Lloves J, Martínez-García MC, Effects of TGFβ1, PDGF-BB, and bFGF, on human corneal fibroblasts proliferation and differentiation during stromal repair, *Cytokine* 96 (2017) 94–101. [PubMed: 28390267]
- [47]. Tiede S, Ernst N, Bayat A, Paus R, Tronnier V, Zechel C, Basic fibroblast growth factor: a potential new therapeutic tool for the treatment of hypertrophic and keloid scars, *Ann. Anat* 191 (1) (2009) 33–44. [PubMed: 19071002]
- [48]. Galie PA, Westfall MV, Stegemann JP, Reduced serum content and increased matrix stiffness promote the cardiac myofibroblast transition in 3D collagen matrices, *Cardiovasc. Pathol* 20 (6) (2011) 325–333. [PubMed: 21306921]
- [49]. Galie PA, Stegemann JP, Simultaneous application of interstitial flow and cyclic mechanical strain to a three-dimensional cell-seeded hydrogel, *Tissue Eng. Part C, Methods* 17 (5) (2011) 527–536. [PubMed: 21174633]
- [50]. Charpentier MS, Conlon FL, Cellular and molecular mechanisms underlying blood vessel lumen formation, *Bioessays* 36 (3) (2014) 251–259. [PubMed: 24323945]
- [51]. Visser CA, Left ventricular remodelling after myocardial infarction: importance of residual myocardial viability and ischaemia, *Heart* 89 (10) (2003) 1121–1122. [PubMed: 12975390]
- [52]. Visser CA, Kan G, Meltzer RS, Koolen JJ, Dunning AJ, Incidence, timing and prognostic value of left ventricular aneurysm formation after myocardial infarction: a prospective, serial echocardiographic study of 158 patients, *Am. J. Cardiol* 57 (10) (1986) 729–732. [PubMed: 3962858]
- [53]. Matsumura Y, Zhu Y, Jiang H, D’Amore A, Luketich SK, Charwat V, Yoshizumi T, Sato H, Yang B, Uchibori T, Healy KE, Wagner WR, Intramyocardial injection of a fully synthetic hydrogel attenuates left ventricular remodeling post myocardial infarction, *Biomaterials* 217 (2019) 119289. [PubMed: 31254935]

- [54]. Yoshizumi T, Zhu Y, Jiang H, D'Amore A, Sakaguchi H, Tchao J, Tobita K, Wagner WR, Timing effect of intramyocardial hydrogel injection for positively impacting left ventricular remodeling after myocardial infarction, *Biomaterials* 83 (2016) 182–193. [PubMed: 26774561]
- [55]. Bhana B, Iyer RK, Chen WL, Zhao R, Sider KL, Likhitanichkul M, Simmons CA, Radisic M, Influence of substrate stiffness on the phenotype of heart cells, *Biotechnol. Bioeng* 105 (6) (2010) 1148–1160. [PubMed: 20014437]
- [56]. Garbern JC, Minami E, Stayton PS, Murry CE, Delivery of basic fibroblast growth factor with a pH-responsive, injectable hydrogel to improve angiogenesis in infarcted myocardium, *Biomaterials* 32 (9) (2011) 2407–2416. [PubMed: 21186056]
- [57]. Shao ZQ, Takaji K, Katayama Y, Kunitomo R, Sakaguchi H, Lai ZF, Kawasuji M, Effects of intramyocardial administration of slow-release basic fibroblast growth factor on angiogenesis and ventricular remodeling in a rat infarct model, *Circ. J* 70 (4) (2006) 471–477. [PubMed: 16565567]
- [58]. Wang H, Zhang X, Li Y, Ma Y, Zhang Y, Liu Z, Zhou J, Lin Q, Wang Y, Duan C, Wang C, Improved myocardial performance in infarcted rat heart by co-injection of basic fibroblast growth factor with temperature-responsive chitosan hydrogel, *J. Heart Lung Transplant* 29 (8) (2010) 881–887. [PubMed: 20466563]
- [59]. Zhu H, Li X, Yuan M, Wan W, Hu M, Wang X, Jiang X, Intramyocardial delivery of bFGF with a biodegradable and thermosensitive hydrogel improves angiogenesis and cardio-protection in infarcted myocardium, *Exp Ther Med* 14 (4) (2017) 3609–3615. [PubMed: 29042955]
- [60]. Kumagai M, Minakata K, Masumoto H, Yamamoto M, Yonezawa A, Ikeda T, Uehara K, Yamazaki K, Ikeda T, Matsubara K, Yokode M, Shimizu A, Tabata Y, Sakata K Minatoya, A therapeutic angiogenesis of sustained release of basic fibroblast growth factor using biodegradable gelatin hydrogel sheets in a canine chronic myocardial infarction model, *Heart Vessel* 33 (10) (2018) 1251–1257.
- [61]. Fathi E, Nassiri SM, Atyabi N, Ahmadi SH, Imani M, Farahzadi R, Rabbani S, Akhlaghpour M Sahebjam M. Taheri, Induction of angiogenesis via topical delivery of basic-fibroblast growth factor from polyvinyl alcohol-dextran blend hydrogel in an ovine model of acute myocardial infarction, *J. Tissue Eng. Regen. Med* 7 (9) (2013) 697–707. [PubMed: 22674791]
- [62]. Tous E, Ifkovits JL, Koomalsingh KJ, Shuto T, Soeda T, Kondo N, Gorman JH 3rd, Gorman RC, Burdick JA, Influence of injectable hyaluronic acid hydrogel degradation behavior on infarction-induced ventricular remodeling, *Biomacromolecules* 12 (11) (2011) 4127–4135. [PubMed: 21967486]
- [63]. MacArthur JW Jr., Purcell BP, Shudo Y, Cohen JE, Fairman A, Trubelja A, Patel J, Hsiao P, Yang E, Lloyd K, Hiesinger W, Atluri P, Burdick JA, Woo YJ, Sustained release of engineered stromal cell-derived factor 1-alpha from injectable hydrogels effectively recruits endothelial progenitor cells and preserves ventricular function after myocardial infarction, *Circulation* 128 (11 Suppl 1) (2013) S79–S86. [PubMed: 24030424]



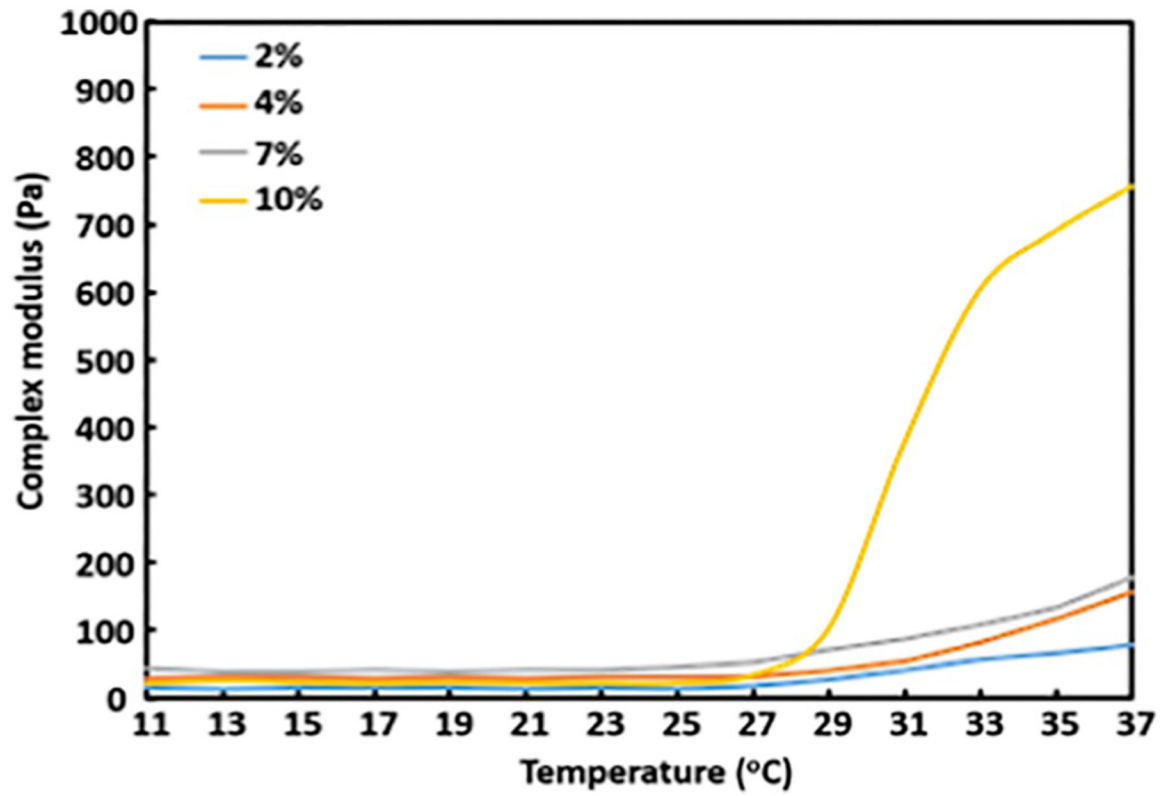
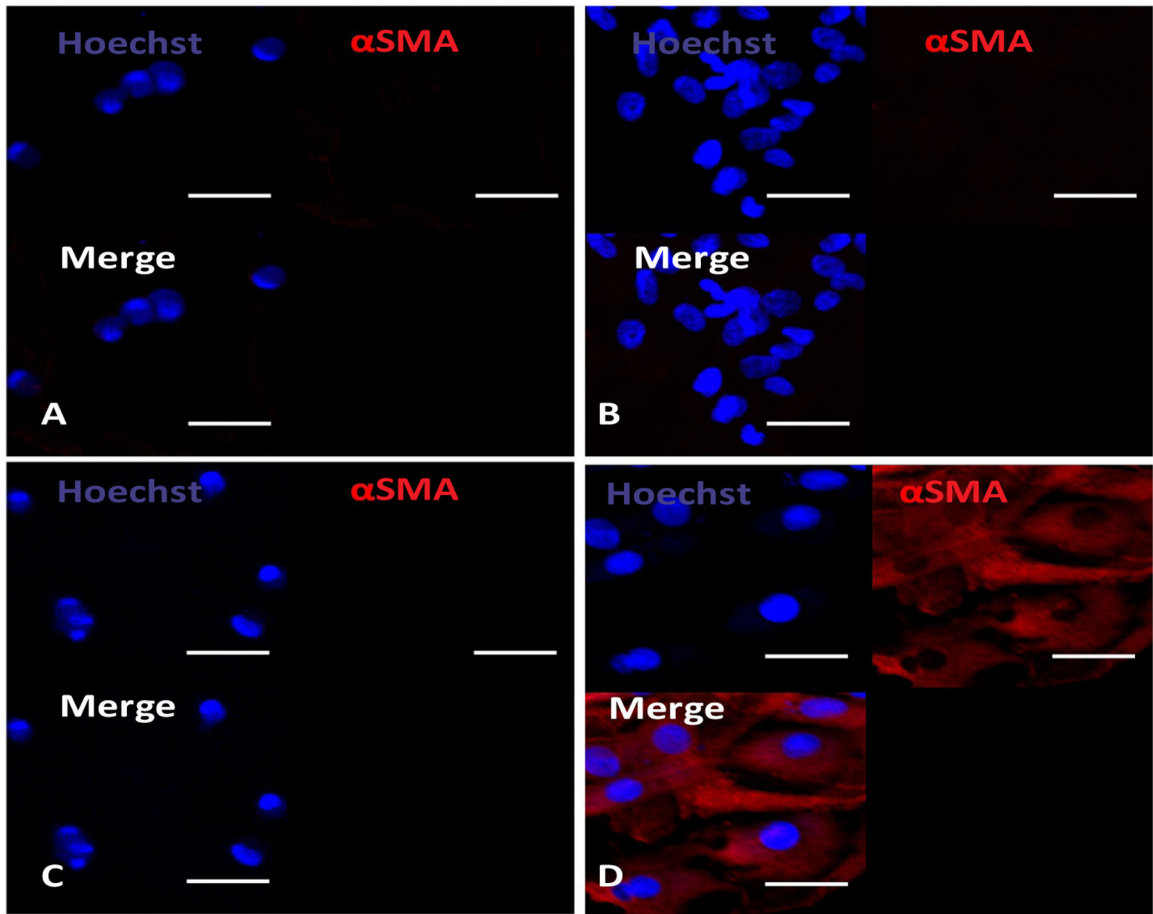
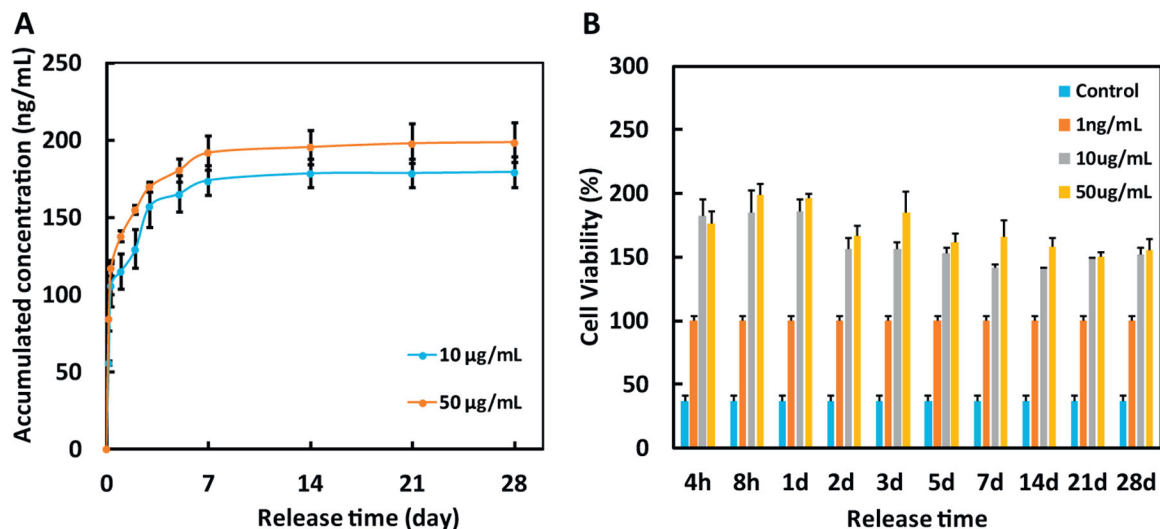


Fig. 1. Rheological characterization of the hydrogel with different concentrations.



**Fig. 2.** Immunohistochemical staining of rat cardiac fibroblasts cultured on the hydrogels with four different concentrations, 2% (A), 4% (B), 7% (C), and 10% (D), for 1 day. Scale bar = 30  $\mu$ m.



**Fig. 3.** (A) Release kinetics of bFGF encapsulated in the 4% hydrogel for 28 days. bFGF loading was 10 and 50 µg/mL, respectively; and (B) Bioactivity of the released bFGF. Non-bFGF containing medium and 1 ng/mL bFGF were utilized as controls. The stimulatory effect of bFGF on cell growth was determined by normalizing MTT absorbance of the release medium to that of the 1 ng/mL bFGF.

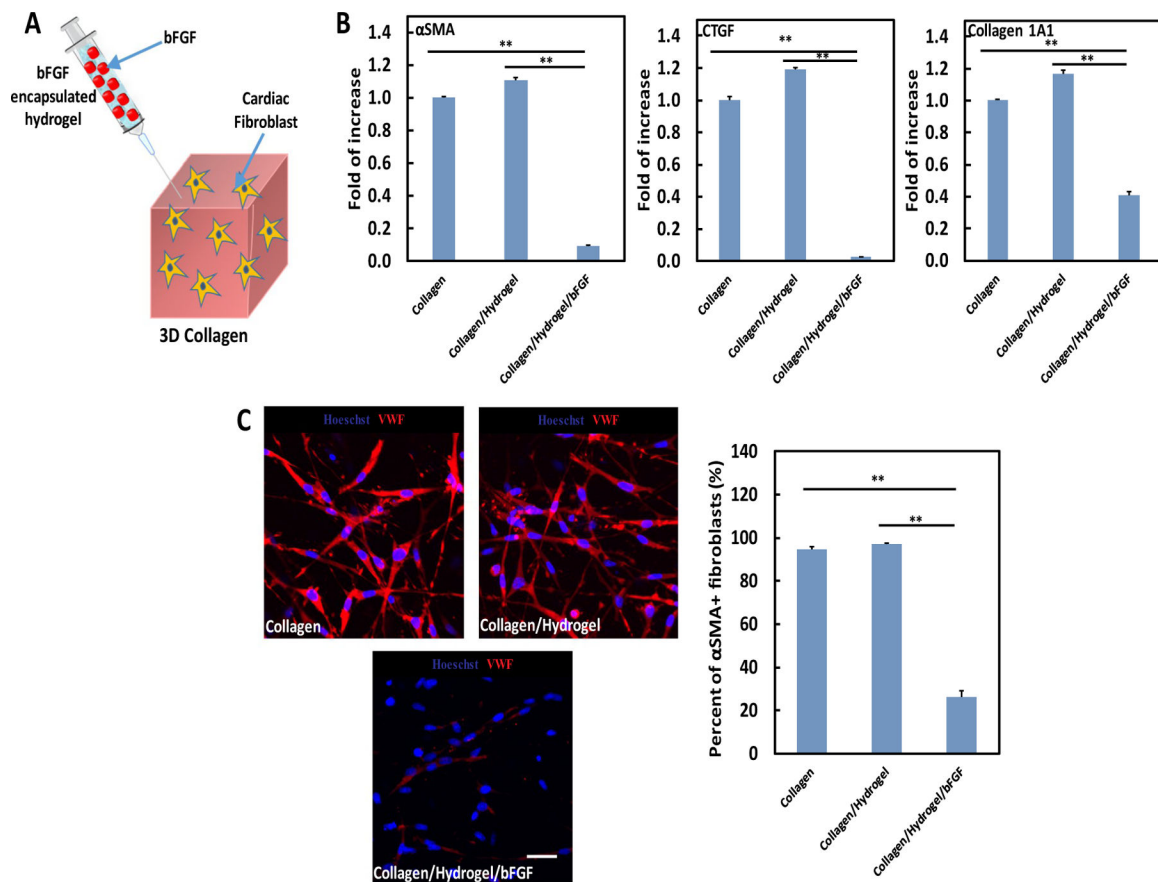


**Fig. 4.**

(A) schematic illustration of 3D collagen model seeded with cardiac fibroblasts and injected with hydrogel/bFGF to study cardiac fibroblast phenotype; (B) gene expression of fibrotic markers ( $\alpha$ SMA, CTGF, and Collagen 1A1) in cardiac fibroblasts; (C) protein expression of fibrotic markers ( $\alpha$ SMA) in cardiac fibroblasts. The cells were cultured for 1 days under within 3D model under hypoxic condition (1%  $O_2$ , 5%  $CO_2$ , and  $37^\circ C$ ) mimicking that of the infarcted heart. 5 ng/ml TGF $\beta$  was used for the culture. Scale bar = 40  $\mu m$ . \*\* $p < .01$ .

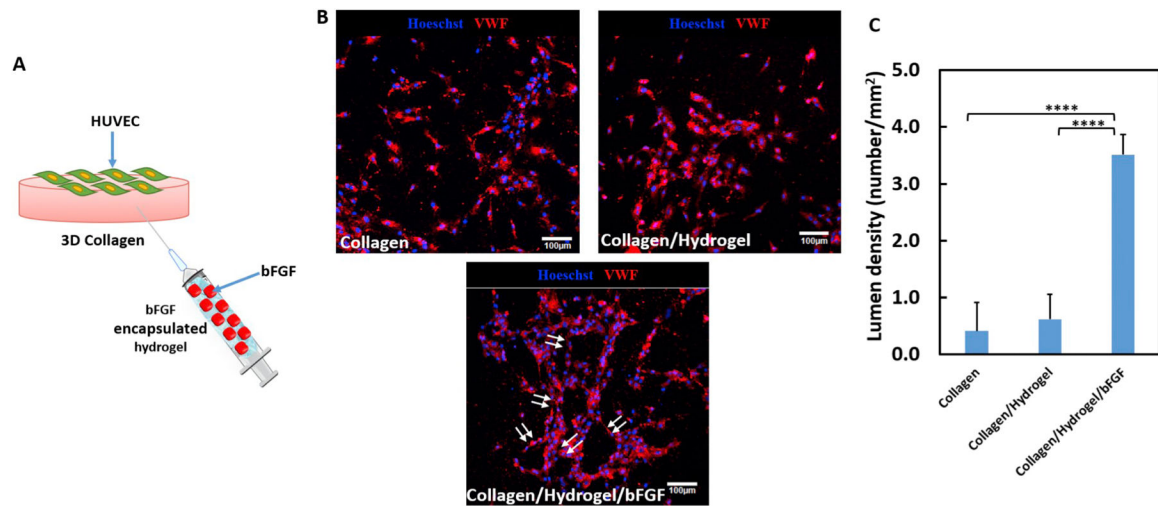


**Fig. 5.** (A) schematic illustration of collagen model seeded with HUVECs on surface and injected with hydrogel/bFGF in the bulk to study endothelial cell morphogenesis; (B) HUVECs formed neovessel (arrowed) under the effect of for 2 days. HUVECs were cultured on the collagen gel surface at hypoxic condition (1% O<sub>2</sub>, 5% CO<sub>2</sub>, and 37°C). 5 ng/mL of TGFβ1 was added. Scale bar = 100 μm. Lumen density was measured from the images. \*\*\*\*  $p < .0001$ .

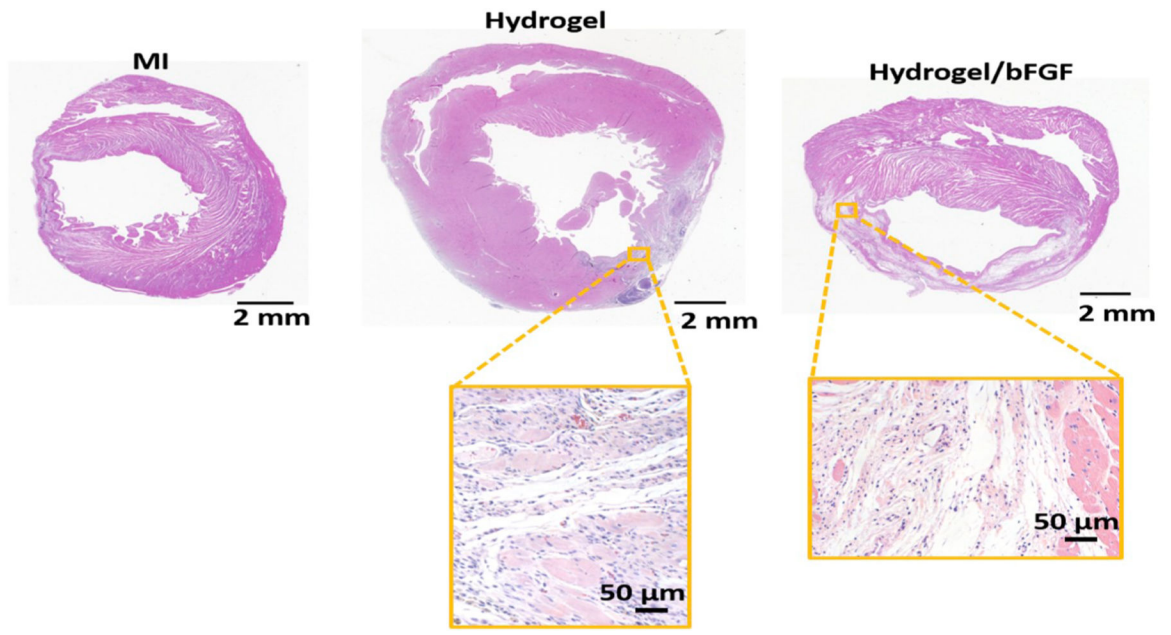


**Fig. 6.** H&E staining of cardiac tissue after 4 weeks of injection with bFGF release system.

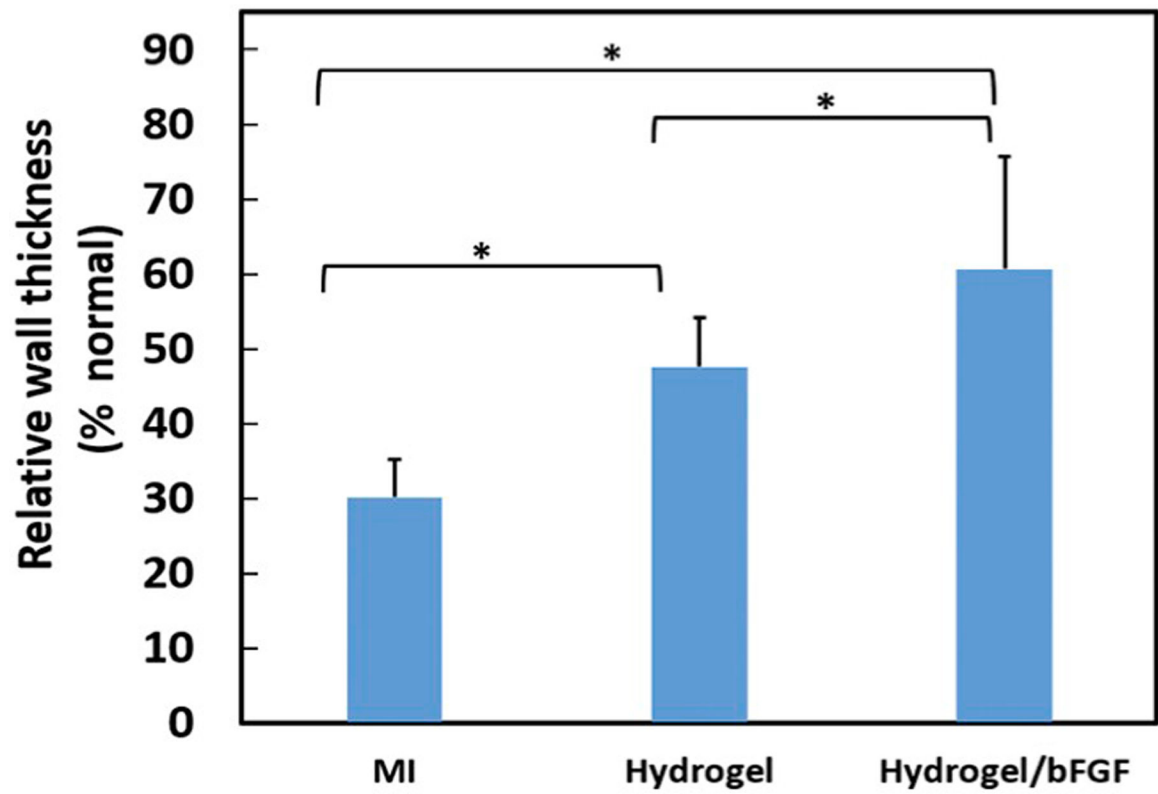


**Fig. 7.** Wall thickness of the myocardium 4 weeks after surgery. The relative wall thickness was evaluated as a ratio between the thickness of myocardium at infarct site to the normal area. \*  $p < .05$ .

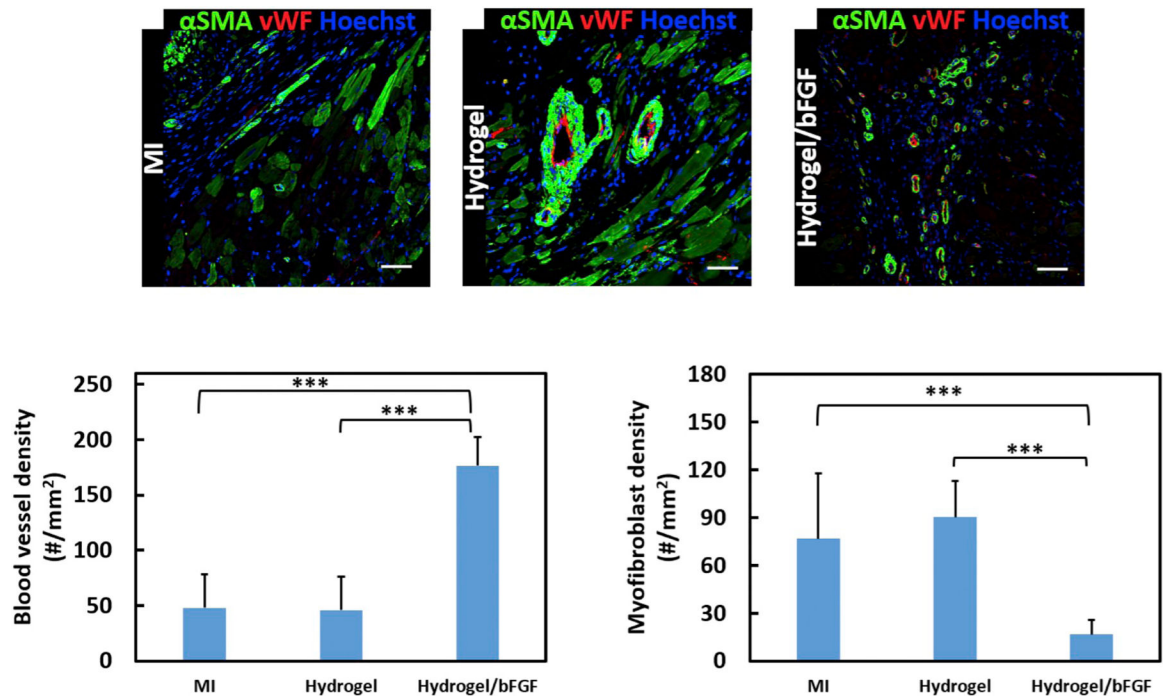


**Fig. 8.** vWF and αSMA staining of the infarcted region after 4 weeks of injection. Scale bar = 50 μm. Myofibroblast and blood vessel density are determined from immunohistological images for MI, Hydrogel, and Hydrogel/bFGF groups. \*\*\* $p < .001$ .



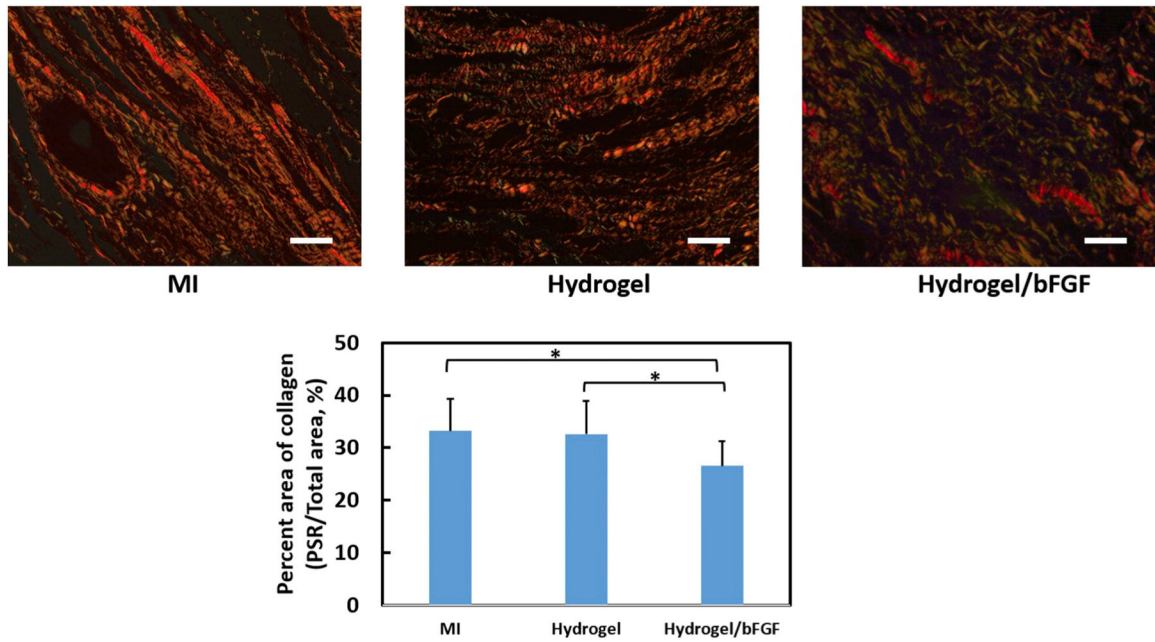


**Fig. 9.** Picosirius red staining of the hearts harvested 4 weeks after surgery. Views were taken at the infarcted region of the MI, Hydrogel, and Hydrogel/bFGF groups. Scale bar = 40  $\mu$ m. Total area of collagen has been quantified from the images. \* $p < .05$ . (For interpretation of the references to colour in this figure legend, the reader is referred to the web version of this article.)

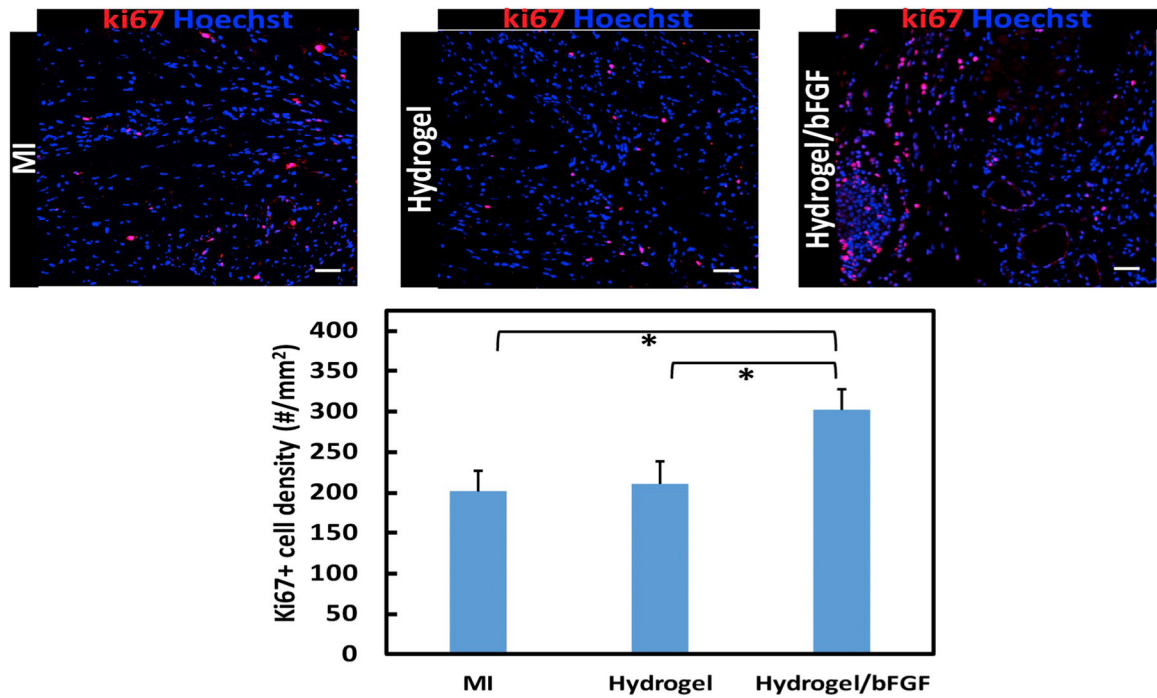


**Fig. 10.** Ki67 staining of the infarcted region after 4 weeks of injection. Scale bar = 100  $\mu$ m. Cell proliferation is identified by ki67 (Red) positive cells density analyzed from images for MI, Hydrogel, and Hydrogel/bFGF groups. \**p* < .05. (For interpretation of the references to colour in this figure legend, the reader is referred to the web version of this article.)

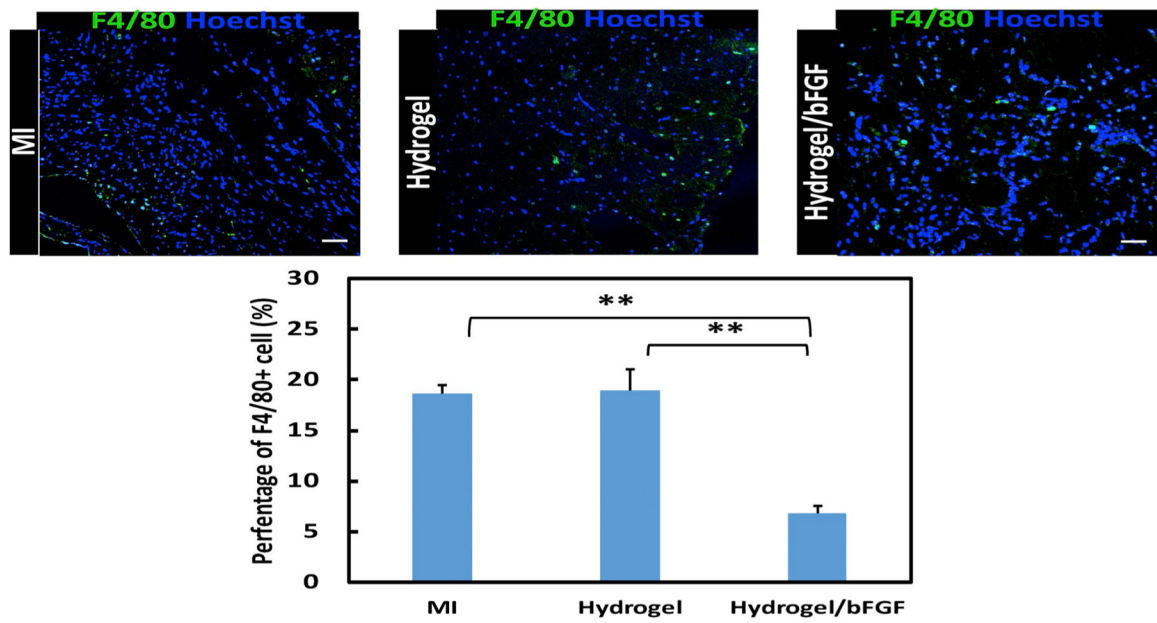


**Fig. 11.** F4/80 staining of the infarcted region after 4 weeks of injection. Scale bar = 100  $\mu$ m. Inflammatory cells are identified by F4/80(Green) positive cells from images for MI, Hydrogel, and Hydrogel/bFGF groups. \*\* $p < .01$ . (For interpretation of the references to colour in this figure legend, the reader is referred to the web version of this article.)

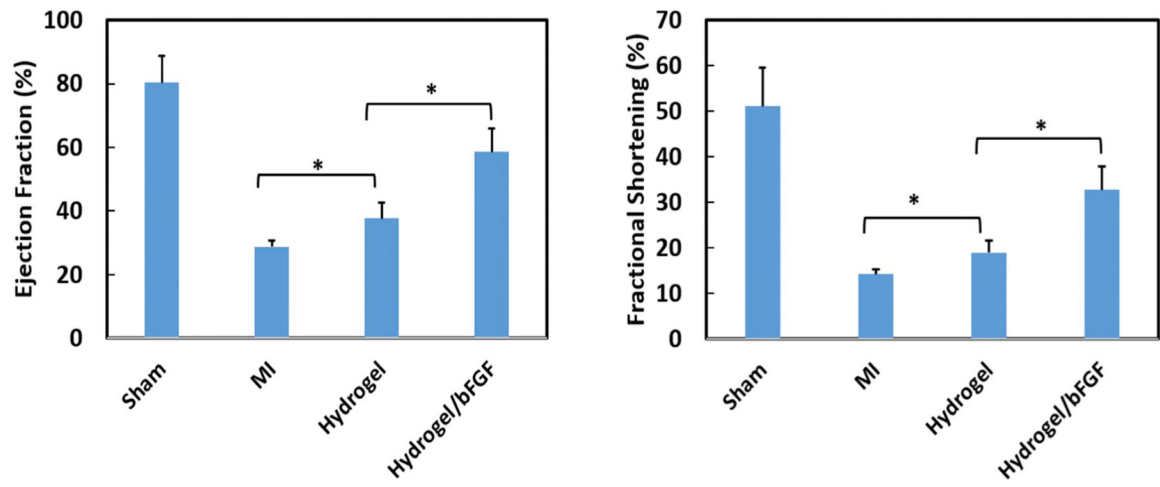


**Fig. 12.** Echocardiographic analysis of four different groups. (a) ejection fraction and (b) fractional shortening. \* $p < .05$ .